

# Online learning and stimulus-driven responses of neurons in visual cortex

Huajin Tang · Haizhou Li · Zhang Yi

Received: 26 February 2010 / Revised: 3 November 2010 / Accepted: 4 November 2010 / Published online: 1 December 2010  
© Springer Science+Business Media B.V. 2010

**Abstract** In understanding how visual scene is processed in visual cortex, it has been an intriguing problem for theoretical and experimental neuroscientists to examine the relationship between visual stimuli and the induced responses of visual cortex. In particular, it is less explored whether and how the collective responses of visual neurons are patterned to reflect the geometrical regularities. In this paper, through a computation model and statistical analysis, we show that the orientation preference maps induced from correlated visual stimuli exhibit geometrical regularities similar as observed in natural images.

**Keywords** Online learning · Stimulus-driven responses · Visual cortex · Orientation preference · High-order statistics

## Introduction

One of the most difficult problems that the visual system has to solve is to group different elements of a scene into

individual objects. Despite its computational complexity, this process is normally effortless, spontaneous, and unambiguous in biological neural systems. It is a fantastic scientific challenge of our time to understand how the visual system analyzes sensory information. The vision research also has a significant impact as it has a wide range of applications including assisting impaired people with vision problems and adding a significant ease in computer vision and robotics control.

The first step in vision is the focusing of light by the lens of the eye to the retina, the impinging light excites the photoreceptors and in turn activates the different types of retinal neurons. The signals are then accumulated and transmitted through the optic nerve and an area of thalamus called the lateral geniculate nucleus (LGN), before the information is transmitted to the primary visual cortex (V1). V1 is the first area of the cortex that process visual information. The topographic organization of the retinal is preserved in both the thalamus and in V1. However, the receptive fields are different: Neurons in the LGN still have a center-surround response character similar to their retinal counterparts, while neurons in V1 respond best to bars of lights of a particular orientation (Kandel et al. 2000).

Experimental techniques can provide information at the scale of a single neuron by using micro-electrodes. The modern optical imaging technique is able to obtain information at the scale of the whole visual cortex, giving rise to intricate global patterns of orientation preference, referred as the orientation preference map (OPM). The distinct features in the mammalian visual cortex are: the preferred orientation of neurons varies continuously across most of the cortex, and there are singularities around which all orientations are present (Blasdel 1992; Horton and Adams 2005).

It is widely believed that visual systems are optimized for the visual properties of the environment inhabited by

---

H. Tang (✉) · H. Li  
Institute for Infocomm Research, A\*STAR,  
Singapore 138632, Singapore  
e-mail: htang@i2r.a-star.edu.sg

H. Li  
Department of Computer Science and Statistics,  
University of Eastern Finland, 80101 Joensuu, Finland  
e-mail: hli@i2r.a-star.edu.sg

Z. Yi  
College of Computer Science, Sichuan University,  
610065 Chengdu, China  
e-mail: zhangyi@scu.edu.cn

the organism. For example, the power spectrum analysis for natural images shows that horizontal and vertical orientations have slightly higher power because of their predominance in natural scenes. In the OPM of cat V1, a larger area of V1 is preferentially activated by vertical and horizontal contours than by contours at oblique orientations (Dragoi et al. 2001).

The study of correlations of a pair of such lines with their relative location in space, indicate a tendency towards co-circularity (Sigman et al. 2001; Geisler et al. 2001). A second rule is that segments are less likely to be integrated with increasing distance between them. A large body of anatomical and electrophysiological research has shown that the V1 intra-cortical connectivity is correlated with orientation preference. The general trend is that long range projections connect neurons with similar orientation preference (Bosking et al. 1997; Kisvarday et al. 1997). These lateral connections are longer and stronger along an axis in the map of visual field that corresponds to the preferred orientation. Statistical analysis for animal's OPMs also illustrated the anisotropic features (Lee et al. 2003) (see also Lee and Kardar 2006), where a high-order statistical property, the reduced symmetry (orientation difference between any pair of cells depends on their topographic relation), was reported. A recent study also provides similar findings for the cortical maps of cats (Hunt et al. 2009).

In this work, a computational model is developed to study the stimulus-driven patterns of visual development. In addition to the findings on the experimental maps (Lee et al. 2003), this study confirms the fact that the OPMs induced by correlated visual stimuli are organized in a geometrical meaningful way: The structure of OPMs developed by correlated input features follows the co-circularity rule in the natural image statistics.

### The model and online learning

Since the early 1990s, computational models have become a prevailing tool to probe into the mechanisms of pattern formation and development of visual maps, such as orientation preference, ocular dominance (Obermayer et al. 1990, 1992; Wolf and Geisel 1998, 2003; Wolf 2005). In the history of modeling visual cortex, an important idea arised, i.e., dimension-reduction mapping (Durbin et al. 1989). In this framework, each point in a high-dimensional feature space (characterized by retinotopic position, orientation, ocular dominance) can be mapped to a corresponding cell on the surface of the cortex (Swindale 1996).

In the dimension reduction framework, Durbin et al. (1989) proposed a computational model called the elastic net to simulate the formation of cortical maps. The behavior of the model is described as follows. Let

$\mathbf{y}_j = (x, y, r, \theta)$  be a vector of cortical cell  $j$ , i.e., the receptive field of cell  $j$ , where  $(x, y)$  is the centre of the receptive field in visual space, and the polar coordinates  $(r, \theta)$  encode preferred orientation  $\theta/2$  and strength of orientation tuning  $r$ , often set to be a constant. In computation, the Cartesian form  $(r \cos \theta, r \sin \theta)$  of  $(r, \theta)$  is actually used. Random stimuli  $\mathbf{x}$  were drawn from the same 4-D space, with  $(x, y)$  uniform in  $[0, 1]$ ,  $\theta$  uniform in  $[0, \pi/2]$ . The activity level of each cortical cell  $j$  in response to each input stimulus  $\mathbf{x}_i$  is calculated using Gaussian receptive fields:

$$W_{ij} = \exp\left(-\frac{\|\mathbf{x}_i - \mathbf{y}_j\|^2}{2K^2}\right) \quad (1)$$

where  $K$  is a distance scaling parameter, also referred to the size of receptive field. This activity is then normalized by dividing by the sum of the responses of all the cortical cells to stimulus  $i$ :

$$w_{ij} = \frac{W_{ij}}{\sum_p W_{ip}} \quad (2)$$

where the summation over  $p$  is over all the cortical cells. This normalization is important to the operation of the system in that it ensures each input stimulus evokes the same amount of responses in the cortex. The receptive field of each cortical cell  $j$  is then evolved towards the stimulus in proportion to its response to that stimulus:

$$\Delta \mathbf{y}_j = \alpha \sum_i w_{ij} (\mathbf{x}_i - \mathbf{y}_j) + \beta K \sum_{j' \in N(j)} (\mathbf{y}_{j'} - \mathbf{y}_j) \quad (3)$$

where  $N(j)$  refers to the set of the neighbours of unit  $j$  in the cortical sheet. In the above adaptation, while the first term allows all the stimuli to be captured by each cortical cell, the second term plays the role of smoothing (neighbouring cells in the cortex have similar response properties). This equation satisfies the two requirements in the animal cortical map development: coverage (the cortical cells should adequately sample feature space) and smoothness (also implying minimization of wire length in cortex). The two requirements are adjusted by the constants  $\alpha$  and  $\beta$ , respectively.

In most previous computational studies of the elastic net (see, e.g., Carreira-Perpinan et al. 2005), a batch mode learning was used based on Eq. 3, in which the whole ensemble of the input stimuli (evenly distributed points in high dimensional feature space, see in next section) was applied to update the response  $\mathbf{y}_j$  for each  $K$ . However, the batch learning is not able to capture the correlation relations between different feature points when the input stimuli contain intrinsic geometrical features such as a natural image. Hence, the online learning algorithm is needed.

From the optimization point of view, the above update equation of  $\mathbf{y}$  is actually minimizing an energy function  $E$  as defined in Durbin and Mitchison (1990):

$$E = -\alpha K \sum_i \log \sum_j \exp\left(-\frac{\|\mathbf{x}_i - \mathbf{y}_j\|^2}{2K^2}\right) + \frac{\beta}{2} \sum_{j \in N(j)} \|\mathbf{y}_j - \mathbf{y}_j\|^2 \tag{4}$$

such that  $\Delta \mathbf{y}_j = -K \partial E / \partial \mathbf{y}_j$  as in the gradient optimization regime.

Rather than directly using the update Eq. 3, as the gradient algorithm is limited to very small value of  $K$ , in this work we add a global learning rate  $\eta$  to formulate the online learning rule:

$$\Delta \mathbf{y}_j = \eta \left( \alpha \sum_i w_{ij} (\mathbf{x}_i - \mathbf{y}_j) + \beta K \sum_{j' \in N(j)} (\mathbf{y}_{j'} - \mathbf{y}_j) \right) \tag{5}$$

The learning rate  $\eta$  is an important factor to affect the stability of the online learning, thus its value should be carefully selected. Throughout this paper, we use the online learning algorithm described by Eq. 5.

In the next, we present a qualitative analysis to show how the cortical map is developed via the elastic net dynamics. Based on the results of Wolf and Geisel (1998), there is a differential version for the dynamics of the elastic net, which can be linearized around the origin as

$$\frac{\partial}{\partial t} \mathbf{y}(r) = -\mathbf{y}(r) + \frac{|s|^2}{2K^2} \mathbf{y}(r) - \frac{|s|^2}{4\pi K^4} \int_{R^2} d^2 r' e^{-\frac{(r-r')^2}{4K^2}} \mathbf{y}(r') + \eta \Delta \mathbf{y}(r). \tag{6}$$

where  $r = (x, y)$  denotes the spatial position,  $|s|$  is a parameter related to the stimuli.

It is assumed the cortical map is developed from uniform homogenous states, so that the last term in the right hand of the above equation is neglected, and  $\mathbf{y}(r)$  is not dependent on the spatial position. By taking such simplification, we further reduce the dynamics as

$$\frac{\partial}{\partial t} \mathbf{y}(r) = -\mathbf{y}(r) + \frac{|s|^2}{2K^2} \mathbf{y}(r) - \frac{|s|^2}{4\pi K^4} \mathbf{y}(r) \int_{R^2} d^2 r' e^{-\frac{r'^2}{4K^2}}. \tag{7}$$

The eigenvalue of the reduced dynamics is

$$\lambda = -1 + \frac{|s|^2}{2\sigma^2} - \frac{|s|^2}{4\pi K^4} \int_{R^2} d^2 r' e^{-\frac{r'^2}{4K^2}}. \tag{8}$$

By calculation of the integral,  $\int_{R^2} d^2 r' e^{-\frac{r'^2}{4K^2}} = \pi K^2$ , over the range  $R : 0 \rightarrow +\infty$ , it follows that

$$\lambda = -1 + \frac{|s|^2}{2K^2} - \frac{|s|^2}{4\pi K^4} \cdot \pi K^2 = -1 + \frac{|s|^2}{4K^2}. \tag{9}$$

From the eigenvalue Eq. 9, it can be seen that when  $K < |s|/2$ ,  $\lambda$  will become positive.

The above qualitative analysis shows that when  $K$  decreases from a large value (in the annealing process) to a critical value such that the value of  $\lambda$  increases to positive, then there will be a phase transition (or called bifurcation) so that the cortical map can develop (see section “Numerical simulations” for a detailed example). This dynamic phenomenon is in line with the bifurcation scenario observed in the stimulus-driven model of ocular dominance patterns developed in Scherf et al. (1999). In our computational model studies,  $|s| = 0.08$ , thus  $K^* < 0.04$  will result in the bifurcation, which is consistent with our numerical simulations in which  $K^*$  is found to be about 0.03 (see Figs. 3, 4, Numerical simulations).

### Stimuli and training images

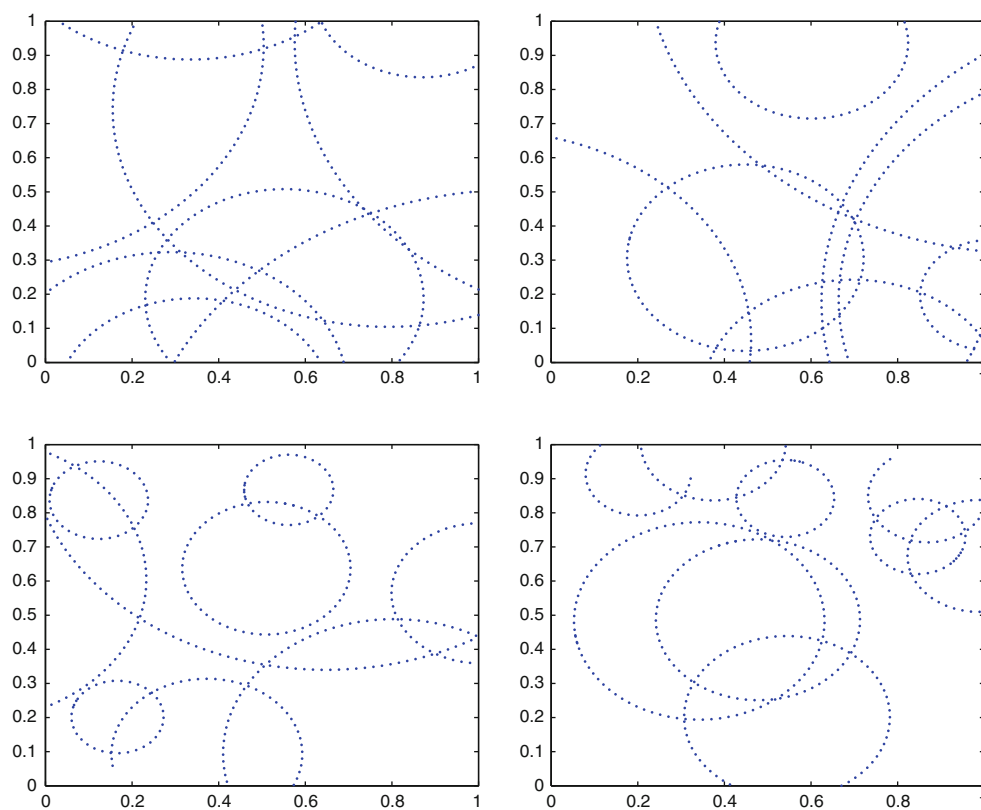
In computational studies of visual cortical map formation, two ways have been used to generate the training set: random distribution (Durbin and Mitchison 1990; Wolf and Geisel 1998) and regular distribution (Carreira-Perpinan et al. 2005). In random distribution, the 4-D stimulus  $\mathbf{x}$ , i.e., a point in the feature space, is randomly sampled from a uniform distribution of feature values. For example, in Durbin and Mitchison (1990), the space position  $(x, y)$  is uniform in a unit square  $[0, 1] \times [0, 1]$ , and the angle  $\theta$  is uniform in  $[0, \frac{\pi}{2}]$ . In the scheme of regular distribution, the visual stimuli are evenly distributed over the feature space. For example, in Carreira-Perpinan et al. (2005),  $(x, y)$  is the grid point of  $20 \times 20$  evenly distributed in the unit square, and  $\theta$  takes all six angles evenly distributed in  $[-\frac{\pi}{2}, \frac{\pi}{2}]$ , thus a total number  $400 \times 6$  of feature points are sampled. However, the two generation methods lack of biological justification, as they do not reflect the universal features of natural images which biological visual system is always exposed to. In natural images, correlated features are universal and unambiguous, e.g., extensive edges and contours, and rule of co-circularity. There have been a lot of studies on characteristics of natural images, and as well as some comparative studies on natural images and cortical maps revealing they are sharing some common features (Dragoi et al. 2001). However, few modeling studies are established to reveal in a direct way that the correlated training stimuli (e.g., the edges and contours from natural images) will drive the responses of visual cortex to develop geometrical regularities. This work attempts to address this concern.

Rather directly using natural images to form the input stimulus set, we use “synthesized images” which consist of lines or curves similar to those in natural images. The advantage of using such synthesized images is that it allows the user to precise control the statistics of the input stimuli while still to preserve the statistics of natural images. Similar method has been used in the work (Rao et al. 2005), which showed that the statistics of such synthesized images matches that of natural images.

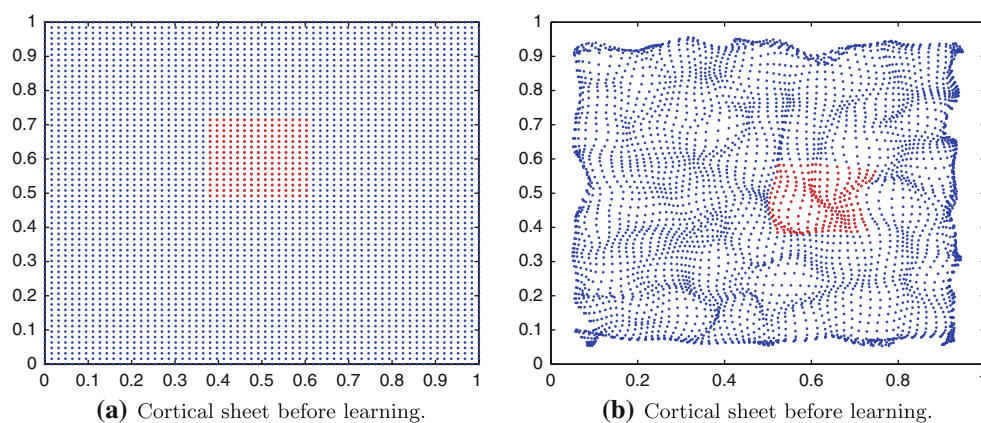
In this work, each synthesized training image consists of several curves, which has a size of  $20 \times 20$ , in line with the visual space size of the regular distribution in Carreira-Perpinan et al. (2005). For each feature point, the selectivity

strength is set as  $r = 0.08$ . A random point and an orientation are chosen in the visual space  $[0, 1] \times [0, 1]$  and in the angle range  $[-\pi/2, \pi/2]$ , and then generate other points subsequently at a separation distance ( $1/64$  is used here) along the curve such that the orientations are tangent to the curve, until a curve is finished. And then repetitively choose a random point and an random orientation to grow a new curve, until generating all points of the training image. As a control, the same visual space positions for all points are kept, but with all different random orientations. The generated curves are dependent on the curvatures, which can be a constant or random different values from a specified range for all curves in one training image.

**Fig. 1** Two methods to generate training images with curves. Method 1 (*top panels*): pre-specifying radius from  $[0.1, 1]$  results in more small-curvature curves. Method 2 (*bottom panels*): pre-specifying curvature from  $[1, 10]$  produces more small-radius curves



**Fig. 2** Configuration of cortical cells and visual space. An area of size  $15 \times 15$  in the cortex is mapped to an area in the visual space (highlighted in red)



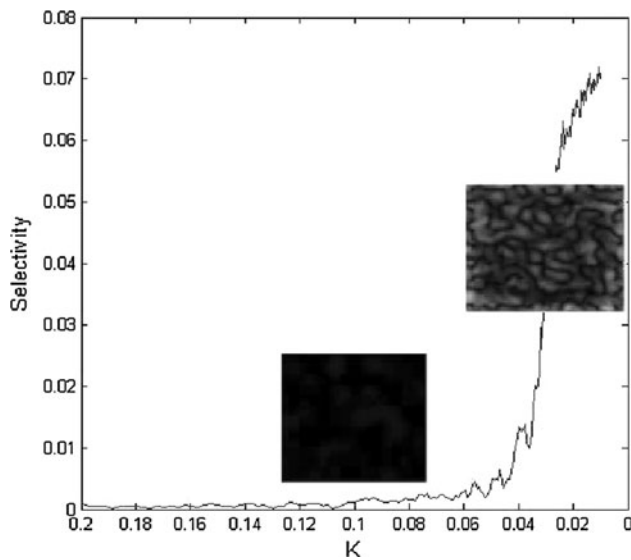


**Fig. 3** Cortical map development through online learning. The input stimuli are drawn from a uniform distribution of feature space, and  $K$  is annealed from 0.2 to 0.01 in 4,000 iterations. The simulation result shows the maximal selectivity strength among all responses of cortical cells at each iteration. It can be seen that the orientation preference patterns developed after  $K$  reached a critical value  $K^*$  ( $K^* \approx 0.03$  in this simulation), as the maximal selectivity of orientation indicates an abrupt change from zero

The training image can be composed of random curvatures, instead of a fixed curvature. We have tried two different methods to randomly choose the curvatures from a uniform distribution: (Method 1) Pre-specify a radius from the range  $[0.1, 1]$  randomly and then draw the points according to the radius; (Method 2) Pre-specify a curvature from the range  $[1, 10]$  and then draw the points according to the curvature. Though the two methods produce the curvatures or radius equivalently in the same range, the resulting distributions of curvature or radius are different, as shown in the appearance of the training images. Method 1 produces the training image with more small-curvatures curves (Fig. 1, top panels), while method 2 produces the training image with more small-radius curves (Fig. 1, bottom panels).

**Numerical simulations**

Different numerical procedures can be used to train the elastic net with uniform distribution and regular distribution stimuli. Based on the update Eq. 3, the solution to minimization of  $E$  at each value  $K$  is found by a Gauss-Seidel procedure (Durbin and Mitchison 1990) or by a more efficient numerical method called Cholesky factorization (Carreira-Perpinan et al. 2005). Different from those numerical methods, we take the gradient based online learning algorithm described by Eq. 5, i.e., the response of

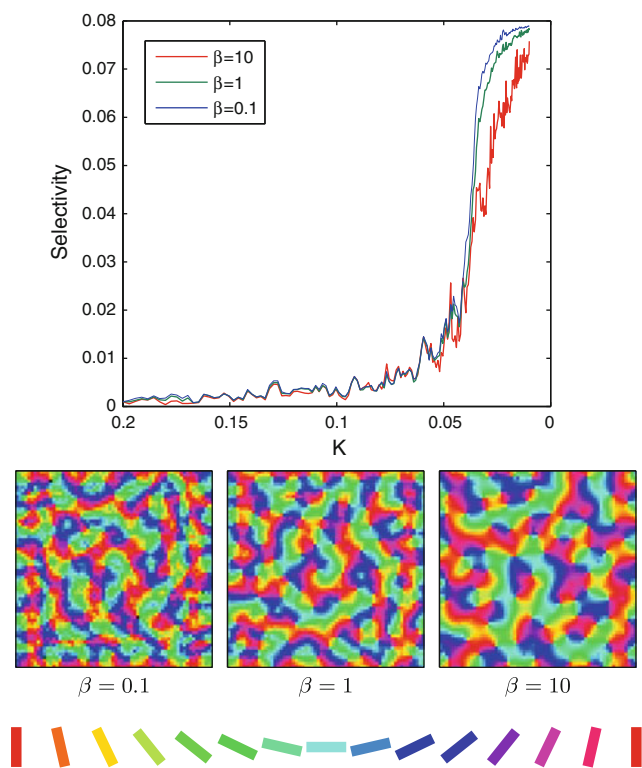


**Fig. 4** Cortical map development through online learning by varying the values of  $\beta$ . The input stimuli are the synthesized images introduced above, and  $K$  is annealed from 0.2 to 0.01 in 4,000 iterations. *Top panel* The simulation result shows the maximal selectivity strength among all responses of cortical cells at each iteration. It can be seen that the bifurcation property with respect to  $K$  is not affected by the values of  $\beta$ . *Bottom panels*. The OP maps from left to right for  $\beta = 0.1, 1, 10$ , respectively. The color key codes the preferred orientations

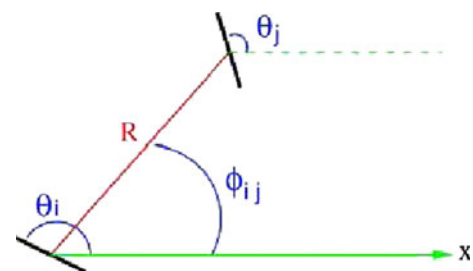


**Fig. 5** The joint histogram used in Lee et al. (2003), of which the first argument is the relative orientation between two pixels  $i$  and  $j$  at a distance  $R, \theta_i - \theta_j$  and the second is the OP of one point measured relative to the line joining the two pixels,  $\phi_{ij} - \theta_j$

cortex cell  $y_j$  adjusts its value according to (5) for a given input stimulus at each iteration.

In this work, the visual space has a size of  $20 \times 20$ , and the cortical space  $64 \times 64$ . The learning rate is 0.1, and the value of  $K$  is annealed from 0.2 to 0.01 in 4,000 iterations. The configuration of the cortical cell is demonstrated in Fig. 2a, where the  $64 \times 64$  grid points represent the cortex

cells, superposed by a unit square of visual space. The receptive fields of cortex cells are initiated by random visual positions. After the cells learn the input stimuli, the receptive field of individual cell becomes selective to one specific position in the visual space, so that all the visual space is covered optimally and the cortex sheet is deformed accordingly as in Fig. 2b.

A typical simulation is shown in Fig. 3, in which the cortical map is developed through the online learning algorithm described above. In online learning, at each step, the responses of cortical cells are adapted to the input

stimulus drawn from a uniform distribution of feature space. The orientation preference map developed after  $K$  reached a critical value  $K^*$  ( $K^* \approx 0.03$  in this example, which is consistent with the critical value of  $K$  for the batch learning with regular distribution input stimuli studied in Carreira-Perpinan et al. 2005).

In 9143practice, the parameter  $\alpha$  in Eqs. 3 and 5 is often normalized to 1, thus the trade-off between coverage and smoothness is mediated only by the parameter  $\beta$ . Through the above qualitative analysis, it is seen that the bifurcation is primarily resulted from the property of the input stimuli,

Fig. 6 The correlation function

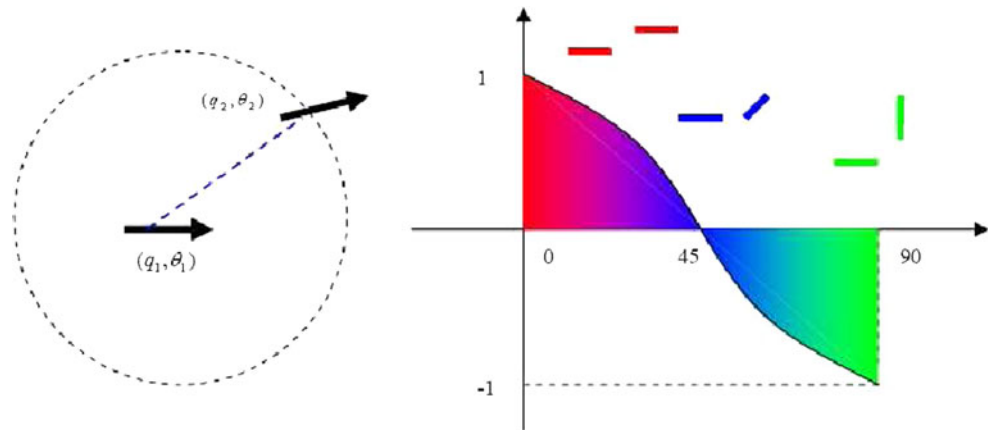
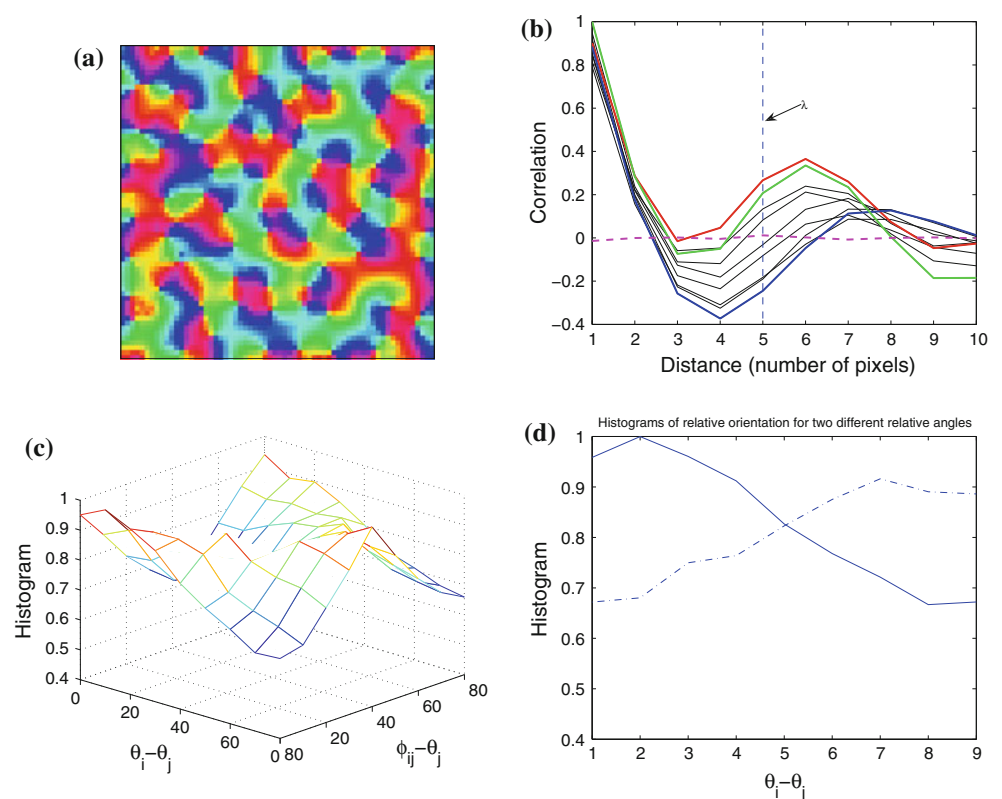


Fig. 7 The orientation map driven by correlated input stimuli and statistical analysis. **a** A typical orientation map. **b** Normalized correlation function values w.r.t. the distance and different relative angle. The red, blue and green lines show relative angles 0, 45, 90 respectively. **c** The full histogram of relative orientation and relative angle at the distance  $\lambda$ . **d** At the distance of  $\lambda$ , the neighboring cortical cells at 0 and 90 degrees of relative angles, the preferred orientations are more likely to be parallel, and at 45 degree, the preferred orientation are more likely to be orthogonal



not the strength of tension  $\beta$ . Extensive simulations by varying different value of  $\beta$  also confirmed the observation: the evolution curve of the maximal selectivity is robust to different values of  $\beta = 0.1, 1, 10$  as shown in Fig. 4, though large  $\beta$  results in large patches of orientations (i.e., orientation columns). Throughout simulations for the following statistical analysis,  $\beta = 10$  is employed.

**Statistical analysis**

Individual neurons in the primary visual cortex have preferential responses to rod-like stimuli of a particular orientation. Oriented segments are abundant in natural images and tend to be collinear or cocircular. It has been an intriguing problem to investigate the relationship between the nature scenes and visual cortical maps, i.e., are the strong geometrical structures in natural images reflected in the visual cortical map?

In Lee et al. (2003), have shown that in the visual cortical maps of monkey and cat, a reduced symmetry (joint rotations of both orientation preference and the underlying topography) exhibits by studying the joint histogram between the relative angle and relative orientation of pairs of points in the OP maps. The calculation of the joint histogram  $h_R[2(\theta_i - \theta_j), 2(\phi_{ij} - \theta_j)]$  is illustrated in Fig. 5

Given a feature vector

$$u = \begin{bmatrix} x \\ y \\ q \cdot \cos(2\theta) \\ q \cdot \sin(2\theta) \end{bmatrix}$$

In an orientation map, the correlation is calculated between the features at different cortical points  $(q_1, \theta_1)$  and  $(q_2, \theta_2)$ . The correlation  $S$  is defined as: positive correlation (+1) if the two orientations are parallel, negative correlation (−1) if the two orientations are perpendicular. The absolute value of  $S$  indicate how close the two orientation are parallel or perpendicular. Here, the correlation function  $S$  is defined by

$$S = q_1 \cdot q_2 \cdot \cos(2\Delta\theta), \tag{10}$$

where  $\Delta\theta$  is the relative orientation between  $\theta_1$  and  $\theta_2$  considered in the range of  $[0, \pi/2]$ . An intuitive illustration of the correlation function is shown by Fig. 6. The correlation function is calculated at different distance and different relative angle for pairs of points in the OPMs.

The statistical analysis results are shown in Figs. 7, 8, and 9. In Fig. 7, the correlation strength is calculated for a range of distance  $R = 1-10$  pixels, and relative angle  $[0, 90]$ . It can be seen that there is a clear dependence of the correlation values upon the distance and relative angle. In particular, the correlation difference at each relative angle (the 9 lines represent the angle from 0 to 90 degree binned at 10 degree) is maximized near the wavelength of the map

**Fig. 8** The orientation map driven by uncorrelated input stimuli and statistical analysis. **a** A typical orientation map trained with uncorrelated features. **b** Normalized correlation function values w.r.t. the distance and different relative angle, showing the control. All the correlations of different relative angles collapsed together, showing no geometrical dependence on relative angle, but the correlations still vary according to separation distance, implying a uniform property in the orientation maps. **c** The joint histogram at the distance  $\lambda$

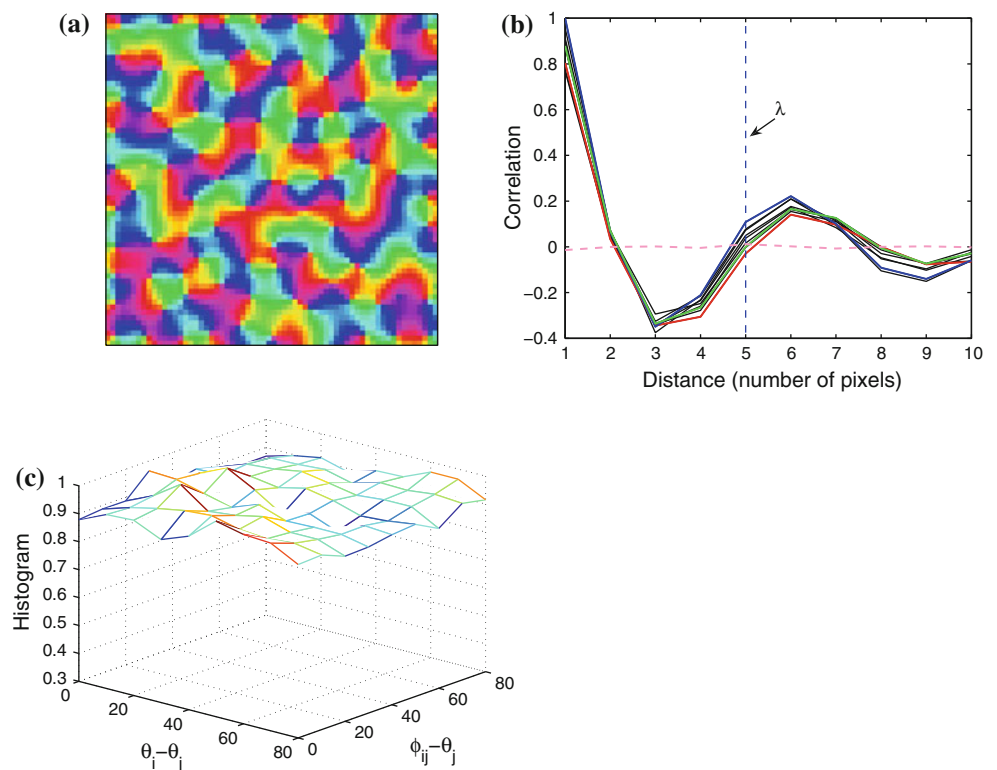
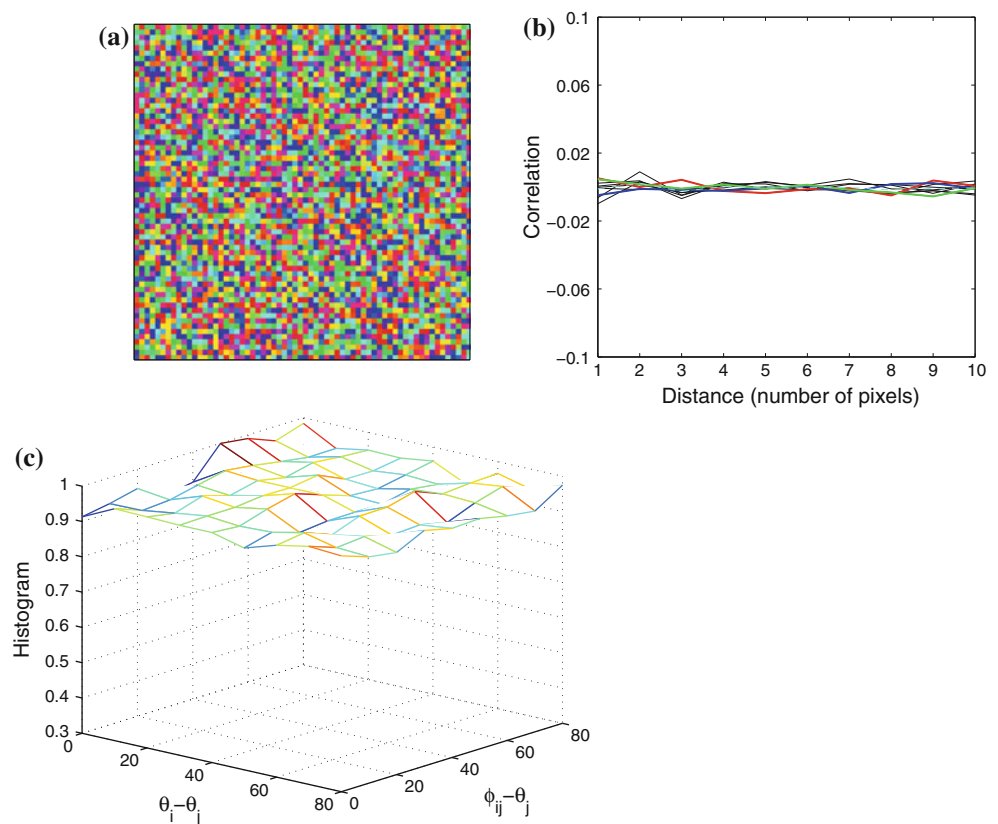


**Fig. 9** The correlation and joint histogram analysis for a random map. The correlation function values reflected no geometrical structure. **a** A random map. **b** Normalized correlation function values w.r.t. the distance and different relative angle. All the correlations of different relative angles collapsed together, and also kept invariant to the distance, showing no any geometrical dependence. **c** The joint histogram at any separation distance is rather flat, not relevant to the orientation difference and relative angle



( $\lambda = 5$  pixels). At this distance, the joint histogram is depicted in the right plot, showing at 0 and 90 degrees of relative angle, more pairs of cells have the same or similar orientation, while at 45 degree, more pairs are orthogonal w.r.t. their orientations. This is in consistent with the co-circularity rule in natural images. While in non-correlated maps (statistics in Fig. 8) and random maps (statistics in Fig. 9), this geometrical structure is not present. The statistical analysis results are in agreement with the studies in Lee et al. (2003) for both a computational model with geometry considerations and a cortical map of monkey. As discussed in Lee et al. (2003), collinearity is a prominent characteristic of line segments in natural images, and thus it is reasonable to expect that orientation preference maps reflect a corresponding tendency.

## Conclusion

In this paper, we have developed a computational model and conducted a statistical analysis to study the stimulus-driven responses of neurons in visual cortex. In this model, the receptive fields of neurons are adapted based on a series of correlated edge segments, an abstract alternative to natural images. We show that the orientation preference maps induced from correlated visual stimuli exhibit

geometrical regularities, in particular, the reduced symmetry and co-circularity tendency, similar as observed in natural images. The results provide further clues to how visual information is processed by the brain.

## References

- Blasdel GG (1992) Orientation selectivity, preference and continuity in monkey striate cortex. *J Neurosci* 12(8):3191–3161
- Bosking WH, Zhang Y, Schofield B, Fitzpatrick D (1997) Orientation selectivity and the arrangement of horizontal connections in tree shrew striate cortex. *J Neurosci* 17(6):2112–2127
- Carreira-Perpinan MA, Lister RJ, Goodhill GJ (2005) A computational model for the development of multiple maps in primary visual cortex. *Cereb Cortex* 15:1222–1233
- Dragoi V, Turcu CM, Sur M (2001) Stability of cortical responses and the statistics of natural scenes. *Neuron* 32:1181–1192
- Durbin R, Mitchison G (1990) A dimension reduction framework for understanding cortical maps. *Nature* 343:644–647
- Durbin R, Szeliski R, Yuille A (1989) An analysis of the elastic net approach to the traveling salesman problem. *Neural Comput* 1:348–358
- Geisler WS, Perry JS, Super BJ, Gallogly DP (2001) Edge co-occurrence in natural images predict contour grouping performance. *Vision Res* 41:711–724
- Horton JC, Adams DL (2005) The cortical column: a structure without a function. *Phil Trans R Soc Lond B* 360:837–862
- Hunt JJ, Giacomantonio CE, Tang H, Mortimer D, Jaffer S, Vorobyov V, Erickson G, Sengpiel F, Goodhill GJ (2009) Natural scene

- statistics and the structure of orientation maps in the visual cortex. *NeuroImage* 47:157–172
- Kandel ER, Schwartz JH, Jessell TM (2000) *Principles of neural science*. 4th edn. McGraw-Hill, New York
- Kisvarday ZF, Toth E, Rausch M, Eysel UT (1997) Orientation-specific relationship between populations of excitatory and inhibitory lateral connections in the visual cortex of the cat. *Cereb Cortex* 7:605–618
- Lee HY, Kardar M (2006) Patterns and symmetries in the visual cortex and in natural images. *J Stat Phys* 125:1247–1270
- Lee HY, Yahyanejad M, Kardar M (2003) Symmetry considerations and development of pinwheels in visual maps. *Proc Natl Acad Sci USA* 100:16036–16040
- Obermayer K, Ritter H, Schulten K (1990) A principle for the formation of the spatial structure of cortical feature maps. *Proc Natl Acad Sci USA* 87:8345–8349
- Obermayer K, Blasdel GG, Schulten K (1992) Statistical-mechanical analysis of self-organization and pattern formation during the development of visual maps. *Phys Rev A* 45(10):7568
- Rao AR, Cecchi G, Peck C, Kozloski J (2005) Evaluation of the effect of input stimuli on the quality of orientation maps produced through self organization. In: Kalviainen H et al (ed) SCIA 2005, LNCS 3540:810–820
- Scherf O, Pawelzik K, Wolf F, Geisel K (1999) Theory of ocular dominance pattern formation. *Phys Rev E* 59(6):6977–6993
- Sigman M, Cecchi GA, Gilbert CD, Magnasco MO (2001) On a common circle: natural scenes and Gestalt rules. *Proc Natl Acad Sci USA* 98:1935–1940
- Swindale NV (1996) The development of topography in the visual cortex: a review of models. *Network* 7:161–247
- Wolf F (2005) Symmetry, multistability and long-range interactions in brain development. *Phys Rev Lett* 95:208701
- Wolf F, Geisel T (1998) Spontaneous pinwheel annihilation during visual development. *Nature* 395:73–78
- Wolf F, Geisel T (2003) Universality in visual cortical pattern formation. *J Physiol-Paris* 97:253–264